Figure S1

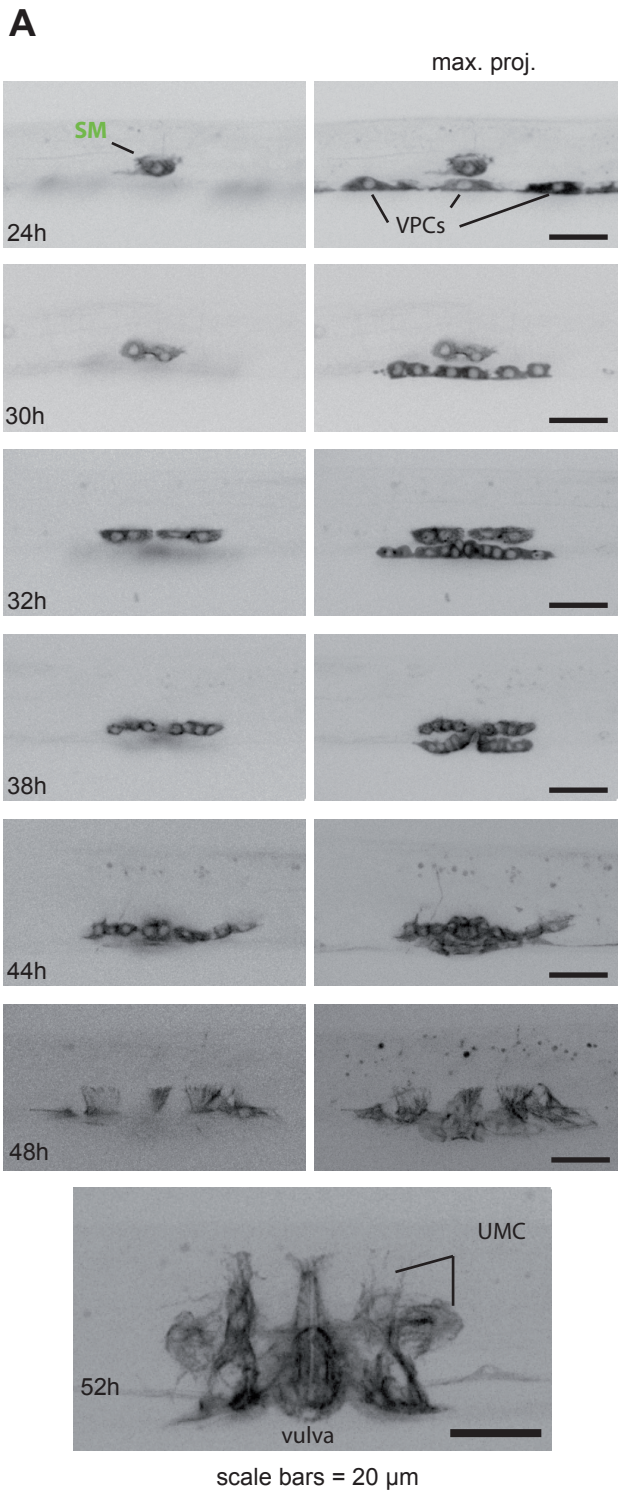

scale bars = 20 μm

Figure S1: Microtubule network visualized in SM lineage during post-embryonic development of *C. elegans*, related to Figure 1.

(A) SM lineage described in Figure 1 followed during post-embryonic development in worms expressing GFP-tagged tubulin under the control of the *unc-62* promoter. Time is in hours from plating starved L1 worms on food. A z-stack through the entire thickness of the worm was acquired using a swept-field real-time confocal microscope. Images are oriented such that anterior is on left and ventral is down. Left: confocal sections containing the left SM. Right: maximal intensity projection of the z-series. Bottom: a maximal intensity projection of *unc-62p*>GFP::tubulin in an adult worm. SM: sex myoblast; VPC: vulval precursor cells; UMC: uterine muscle cells. Scale bars = 20 μm. (B-C) Montages of a 1 sec interval time series of cropped area of a single confocal slice in SM (B) and UMC (C). These panels correspond to the dynamics data presented in Figure 1. Kymograph 1 corresponds to a MT tracked for 60 sec (#1) in an SM precursor (SM) extracted from Movie S1. Kymograph 2 corresponds to the MT bundle (#2) imaged in a UMC and kymograph 3 to a single MT in the same cell. Both kymographs represent 90 sec of tracking. Bundled MTs can be recognized in the kymograph by the increased grey value intensity where the two MTs are superimposed. Kymograph 2 and 3 were extracted from Movie S3. Scale bars = 5 μm.

Figure S2

A

Vertical elongation

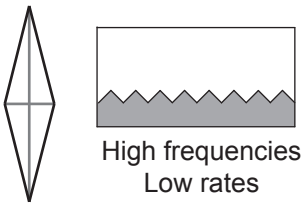

High frequencies
Low rates

Diamond Graphs

rescue frequency
shrinkage rate — growth rate
catastrophe frequency

Equal rates and frequencies

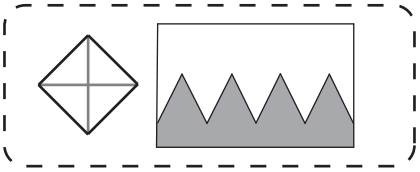

Horizontal elongation

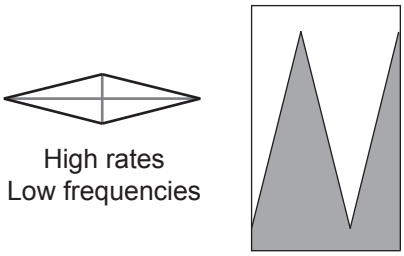

High rates
Low frequencies

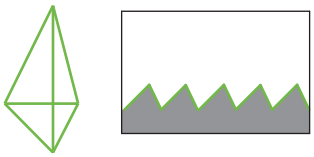

Low growth rate
Rescue freq. > Catastrophe freq.

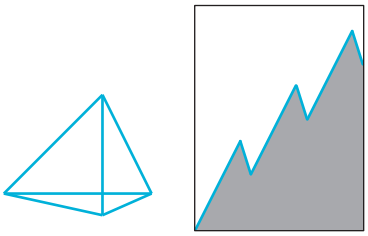

Shrinkage rate > Growth rate
Rescue freq. > Catastrophe freq.

B

Species	*C.elegans*			*Drosophila*	Newt	Rat Kangaroo	Chinese hamster	*Xenopus*					Cowpea	
cell type	SM*	UMC*	1-4 cells zygote*	S2 cells[a]	lung epithelial cells[b]	PtK1[c]	CHO[c]	neuron[d]	interphase extract[e]	mitotic extract[e]	i 218[f]	m 218[f]	Protoplast interphase[g]	Protoplast mitotic[g]
Growth rate (µm/sec)	0,1199	0,1534	0,4144	0,0883	0,12	0,1983	0,3283	0,1767	0,155	0,205	0,3833	0,1633	0,0833	0,1467
Shrinking rate (µm/sec)	0,4493	0,8495	0,3884	0,1883	0,2883	0,33	0,5367	0,1617	0,2133	0,255	0,9167	1,1167	0,3333	0,333
Catastrophe frequency (sec-1)	0,1774	0,0448	0,2011	0,011	0,014	0,054	0,061	0,012	0,018	0,116	0,018	0,116	0,02	0,034
Rescue frequency (sec-1)	0,3188	0,2782	0,2135	0,005	0,044	0,196	0,13	0,029	0,011	0,027	0,011	0,027	0,08	0,08

C

Caenorhabditis elegans*

SM* — UMC* — zygote* — *Drosophila* S2 cells[a] — Newt Lung[b] — PtK_1[c] — CHO[c]

Xenopus

neurons[d] — interphase extract[e] — mitotic extract[e] — clarified interphase[f] — clarified mitotic[f]

Plants

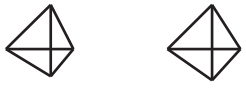

Protoplast interphase[g] — Protoplast mitotic[g]

a, (Li *et al*., 2011) ; b, (Cassimeris *et al*., 1988) ; c, (Shelden and Wadsworth, 1993) ; d, (Tanaka and Kirschner, 1991) ; e, (Belmont *et al*., 1990) ; f, (Parsons and Salmon, 1997) ; g, (Dhonukshe & Gadella, 2003)

Figure S2: Representation and interpretation of microtubule behavior using diamond graphs; related to Figure 1 and Figure 2.

(A) Tutorial representation of MT behavior according to diamond graph shape. A square represents equal rates and equal frequencies, and a length change in any "strut" represents a change in that parameter. The simulated kymographs next to each diamond graph represent the corresponding trend in MT behavior. Green and blue simulated kymographs were created using the experimental data for SM and UMC, respectively (Figure 1 and 2). This non-stochastic simulation predicts that in the UMC, MTs increase in length and that eventually all tubulin is polymeric. This is distinct from the steady-state dynamics seen in the cell, likely because in cells the amount of available tubulin is regulated, and dynamic events are stochastic and controlled by multiple factors (*i.e.* subcellular regulation such as at the cell periphery) not accounted for in this simulation.

(B) Comparison of SM and UMC (Figure 1 and Table 1) with published data[a-f] of MT dynamics in different cell types. (C) Diamond graphs created with published data from (B) of MT dynamics of different cell types allow comparison with *C. elegans* SM, UMC and zygote (*parameters measured in this study, with equal settings). For clarified *Xenopus* extract (218,000xg centrifugation supernatant)[f], catastrophe and rescue frequencies were not available, we thus used these data from non-clarified extract[e] for the diamond graph.

Figure S3

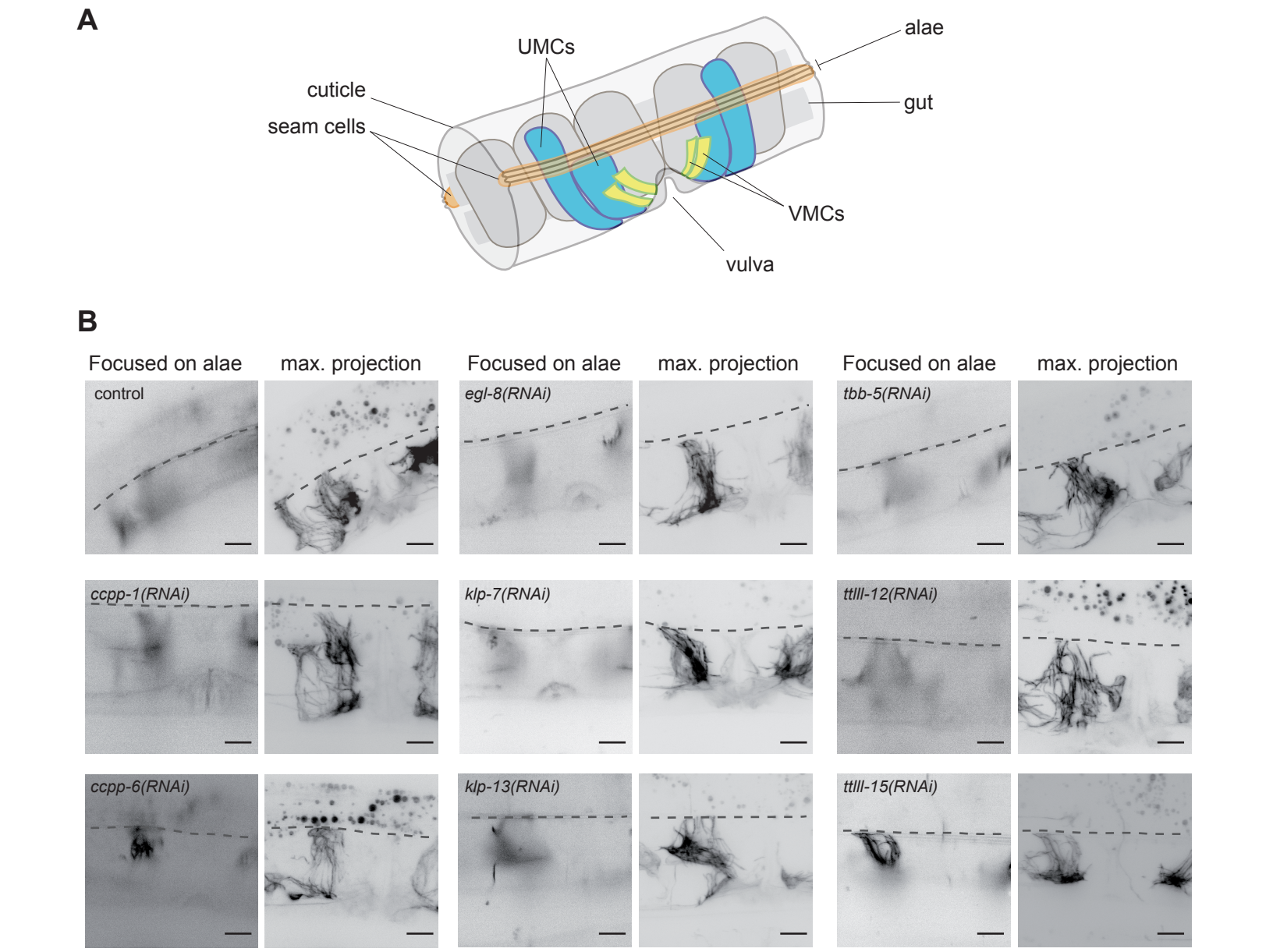

Figure S3: UMC architecture and tissue interactions are preserved in Egl worms, related to Figure 5. (A) Schematic volume view of the egg-laying apparatus in an adult worm. This view correspond to the central section corresponding to the central 1/5th of worm's length. UMCs: Uterine Muscle Cells, VMCs: Vulval Muscle Cells. (B) For every target inducing egg-laying defect (Figure 5), a single confocal plane displaying the location of seam cells (at the alae; dashed line) is represented next to a maximal intensity projection of the full z-stack of the same cell, in *unc-62p*>GFP::tubulin strain. Even though MT organization is affected by these protein depletions, the position of the UMCs within the tissue, and their cell-to cell contacts, are preserved. Scale bars = 20 µm.

Table S1: Microtubule dynamics data in SM and UMCs, related to Figure 1

cell type	SM			UMCs					
population	total			total			on-track		
	mean	SEM	n	mean	SEM	n	mean	SEM	n
Growth rate (µm/sec)	0,12	0,003	121	0,15	0,003	169	0,18	0,004	51
Growth length (µm)	1,10	0,03	121	3,21	0,08	169	2,62	0,11	51
Growth duration (sec)	5,64	0,16	121	22,34	0,56	169	7,11	0,78	51
Shrinking rate (µm/sec)	0,45	0,03	121	0,85	0,02	169	0,91	0,04	51
Shrinking length (µm)	1,47	0,09	121	2,50	0,10	169	1,49	0,10	51
Shrinking duration (sec)	3,14	0,20	121	3,60	0,13	169	3,14	0,22	51
Catastrophe (sec-1)	0,18	0,01	121	0,05	0,001	169	0,07	0,004	51
Catastrophe (µm-1)	0,91	0,03	121	0,31	0,01	169	0,38	0,02	51
Rescue (sec-1)	0,32	0,02	121	0,28	0,01	169	0,32	0,02	51
Rescue (µm-1)	0,68	0,04	121	0,40	0,02	169	0,67	0,05	51

SEM: standard error of the mean. n = number of MTs. n(worms) ≥ 12

Table S2 : Brood size and scored phenotypes in RNAi feeding screen, related to Figure 3

lower case = low penetrance < 1/2

bold > 25% reduction vs. CTRL upper case = high penetrance > 1/2

			Systemic RNAi						Tissue specific RNAi			
			Brood Size (Eggs/day/worm)		Phenotype in MDX12				Phenotype in NK741			
Gene Name	Known Ortholog	Sequence Name	L1 feeding	L4 feeding	Dev.	Pvl	Ste	Egl	Dev.	Pvl	Ste	Egl
L4440 empty vector		-	58,9	57,7								
apr-1	APC	K04G2.8	**38,8**	45,3								
asf-1 / unc-85	ASF1A	F10G7.3	**27,7**	**27,3**								
beta-tubulin cofold. factor D	TBCD-1	F16D3.4	**32,2**	54,7		pvl				pvl		
bmk-1	BimC/kinesin-5	F23D12.8	**38,5**	**21,8**			ste		-	-	-	-
ccpp-1	CCP-1	F56H1.5	**27,7**	**26,8**				egl				
ccpp-6	CCP-6	EEED8.6	**33,3**	**34,7**				egl				egl
cct-6	CCT6A	F01F1.8	**0,0**	**8,0**		PVL	ste			pvl		
ckap-1	CKAP	F53F4.3	49,7	58,3								
cls-1	CLASP	C07H6.3	**24,8**	50,3		pvl				pvl		
cls-2	CLASP	R107.6	**36,0**	56,3								
cls-3	CLASP	ZC84.3	**41,0**	53,7				egl				egl
dhc-1	dynein heavy chain	F21E12.4	**0,0**	**23,5**	DEV	PVL	STE			PVL		egl
dnc-1	p150 dynactin	ZK593.5	**24,7**	**34,7**		pvl	ste			pvl		
ebp-2	EB1/3	VW02B12L.3	**26,0**	**10,5**		pvl						
ect-2	ECT2	T19E10.1	**0,0**	**7,3**		PVL	ste	egl	dev	pvl		egl
efa-6	ARP6 GEF	Y55D9A.1	**23,2**	58,5		pvl						
egl-2	voltage-gated K+ channel	F16B3.1	**32,2**	**27,2**				egl				egl
egl-26	lecithin retinol transferase	C23H3.1	**7,5**	59,0		PVL				pvl		
egl-8	phospholipase C	B0348.4	**17,5**	**23,7**				egl				egl
elp-1	EMAP	F38A6.2	53,5	50,7								
erm-1	ERM	C01G8.5	**11,8**	44,8	dev	pvl				pvl		
figl-1	fidgetin	F32D1.1	**27,0**	**39,2**								
gap-2	RasGAP	ZK899.8	**7,3**	49,2			ste	egl				
Huntingtin-ass. prot. 1	Huntigtin-ass. Protein 1	C33G8.3	**32,2**	**22,2**								egl
klc-1	kinesin light chain	M7.2	47,3	55,3		pvl				pvl		
klp-10	kinesin Klp2/KIF15	C33H5.4	53,5	**31,5**								
klp-11	kinesin-II	F20C5.2	**38,5**	49,5								
klp-12	kinesin like protein	T01G1.1	**39,5**	**28,2**		pvl		egl				
klp-13	kinesin Kip3	T01G1.1	**33,7**	58,8				egl				egl
klp-18	kinesin klp2	C06G3.2	60,5	52,8		pvl				pvl		
klp-7	MCAK	K11D9.1	**27,2**	**18,0**				egl				egl
mec-12	alpha-tubulin	C44B11.3	**39,7**	**38,0**								
mei-1	katanin p60	T01G9.5	51,5	51,8	dev							
mei-2	katanin p80	F57B10.12	**23,0**	**34,8**			ste					
nfm-1	merlin/schwannomin	F42A10.2	**42,2**	**17,5**			ste					
nud-1	nudC	F53A2.4	**0,0**	48,0			ste					
pak-1	PAK1	C09B8.7	**34,7**	**39,2**		pvl		egl		pvl		egl
par-1	PAR1	H39E23.1	**11,5**	**40,3**		pvl		egl		pvl		
pes-7	IQGAP	F09C3.1	56,3	48,8								
plk-1	polo kinase	C14B9.4	**0,0**	73,7	dev	pvl	ste			pvl		
ptl-1	tau	F42G9.9	58,0	**41,3**								
rac-1	RAC1	C09G12.8	**40,7**	47,3		pvl						
sas-3	SAS3	F58A4.8	**0,0**	47,2		PVL		egl		pvl		
sas-4	SAS4	F10E9.8	**1,0**	46,3		pvl	ste			pvl		
sas-6	SAS6	Y45F10D.9	**2,8**	51,5	DEV	PVL				pvl		
snx-1	nexin	C05D9.1	**26,3**	**32,5**		pvl				pvl		
spas-1	spastin	C24B5.2	**31,3**	44,7		pvl						
spd-1	PRC1	Y34D9A.4	50,2	**35,7**		PVL				pvl		
tac-1	TACC	Y54E2A.3	46,2	**18,0**				egl				egl
tag-170	TXNDC9	C05D11.3	**5,7**	**40,8**			ste					
tba-1	alpha-tubulin	F26E4.8	**0,0**	**23,3**	DEV	PVL	ste		dev	PVL	ste	
tba-2/mel-45	alpha-tubulin	C47B2.3	**2,3**	52,3		PVL	ste			PVL	ste	
tba-6	alpha-tubulin	F32H2.9	**0,0**	**3,2**	DEV		ste				ste	
tba-8	alpha-tubulin	ZK899.4	**37,3**	**26,0**								
tbb-1	beta-tubulin	K01G5.7	**0,0**	**20,2**		pvl	ste			pvl		
tbb-2	beta-tubulin	C36E8.5	**0,0**	**30,8**	DEV	pvl	ste			pvl		
tbb-4	beta-tubulin	B0272.1	**16,2**	46,0			ste					
tbb-5	beta-tubulin	C54C6.2	**32,7**	46,3				egl				
tpxl-1	TPX2	Y39G10AR.12	**9,3**	**14,5**		pvl		egl		pvl		
ttll-12	TTLL-12	D2013.9	**37,7**	55,7				egl				
ttll-15	TTLL-15	K07C5.7	**35,7**	56,3				egl				egl
ttll-4	TTLL-4	ZK1128.6	**17,5**	**26,5**		pvl				pvl		
ttll-5	TTLL-5	C55A6.2	53,7	60,2								
vab-10	MACF	ZK1151.1	0,0	62,8	DEV	pvl			dev	pvl		
zen-4	MKLP-1/kinesin-6	M03D4.1	0,0	60,5		PVL	ste			pvl		
zyg-9	XMAP215/TOGp	F22B5.7	53,8	**37,0**								

Table S2 Legend

Alphabetical list of candidates tested for the reduction of brood size in L1 and L4 feeding (Figure 3). Closest known orthologs in *Drosophila*, mammals, *Xenopus* or yeasts are mentioned in the second column depending on the most commonly used name in the literature. Sequence names correspond to the annotation on Wormbase (www.wormbase.org). Number of eggs laid per day and per worm correspond to an average of 3 to 5 worms isolated on a feeding plate after L1- or L4-feeding. Bold numbers represent a significant reduction of the brood size corresponding to less than 0.75 the number of eggs laid per control worms. This arbitrary threshold is voluntarily low and enables reducing false positive. Macroscopic phenotypes were scored using a dissecting scope as shown in Figure 3C and were notified in their respective column with the following abbreviations: Dev (developmental arrest); Pvl (protruded vulva); Ste (sterility); Egl (egg-laying defective). Lowercase and uppercase account for a penetrance of each phenotype being respectively lower than 50% or higher than 50%.

Table S3: Dynamics parameters of UMC in egg-laying defective worms, related to Figure 5

	CCPP-1			CCPP-6			TTLL-12			KLP-13			TBB-5			KLP-7			EGL-8			TTLL-15			CONTROL		
	mean	SEM	n	mean	SEM	n	mean	SEM	n	mean	SEM	n	mean	SEM	n	mean	SEM	n	mean	SEM	n	mean	SEM	n	mean	SEM	n
Growth rate (µm/sec)	0,20	0,004	303	0,14	0,005	259	0,20	0,005	299	0,15	0,01	169	0,15	0,01	180	0,15	0,004	211	0,22	0,01	315	0,18	0,01	215	0,18	0,003	353
Shrinking rate (µm/sec)	0,94	0,03	297	0,84	0,02	225	0,93	0,02	265	0,94	0,03	114	0,69	0,02	206	0,81	0,03	130	0,94	0,02	217	0,88	0,03	188	0,94	0,02	219
Catastrophe frequency (sec-1)	0,08	0,003	303	0,05	0,002	259	0,06	0,002	299	0,05	0,003	169	0,07	0,004	180	0,06	0,003	211	0,06	0,002	315	0,06	0,003	215	0,07	0,002	353
Rescue frequency (sec-1)	0,29	0,01	296	0,24	0,01	225	0,20	0,01	265	0,21	0,01	114	0,27	0,01	206	0,17	0,01	130	0,20	0,01	217	0,25	0,01	188	0,22	0,01	219

SEM: standard error of the mean. n = number of MTs. n(worms) ≥ 8

Table S4: Dynamics parameters of SM and UMC after CLS-1 and KLP-7 depletions, related to Figure 6

CONTROL RNAi (L4440)									
cell type	SM			UMC					
population	total			total			on-track		
	mean	SEM	n	mean	SEM	n	mean	SEM	n
Growth rate (µm/sec)	0,13	0,004	72	0,17	0,004	167	0,19	0,01	87
Growth length (µm)	0,93	0,05	80	3,32	0,10	167	2,23	0,13	87
Growth duration (sec)	5,79	0,30	80	21,08	0,68	167	13,00	0,80	87
Shrinking rate (µm/sec)	0,67	0,06	76	0,93	0,02	269	0,84	0,05	88
Shrinking length (µm)	1,46	0,09	76	2,50	0,09	269	2,21	0,13	88
Shrinking duration (sec)	2,88	0,21	76	3,03	0,12	269	3,24	0,26	88
Catastrophe (sec-1)	0,15	0,01	80	0,05	0,002	167	0,08	0,01	87
Catastrophe (µm-1)	1,07	0,06	80	0,30	0,01	167	0,45	0,03	87
Rescue (sec-1)	0,35	0,03	76	0,33	0,01	269	0,31	0,03	88
Rescue (µm-1)	0,68	0,04	76	0,40	0,01	269	0,45	0,03	88
Time at cortex (sec)				3,8	0,2	159			
CLS-1^{CLASP} (RNAi)									
cell type	SM			UMC					
population	total			total			on-track		
	mean	SEM	n	mean	SEM	n	mean	SEM	n
Growth rate (µm/sec)	0,14	0,01	229	0,15	0,004	242	0,21	0,01	72
Growth length (µm)	0,67	0,03	229	1,55	0,09	242	2,96	0,20	72
Growth duration (sec)	4,83	0,18	229	9,69	0,43	242	14,23	0,95	72
Shrinking rate (µm/sec)	0,81	0,03	194	0,94	0,05	144	1,26	0,09	59
Shrinking length (µm)	1,72	0,07	194	2,65	0,17	144	3,68	0,24	59
Shrinking duration (sec)	2,41	0,10	194	3,08	0,19	144	3,52	0,30	59
Catastrophe (sec-1)	0,21	0,01	229	0,10	0,01	242	0,07	0,01	72
Catastrophe (µm-1)	1,49	0,08	229	0,65	0,04	242	0,34	0,02	72
Rescue (sec-1)	0,42	0,02	194	0,33	0,02	144	0,29	0,02	59
Rescue (µm-1)	0,58	0,02	194	0,38	0,02	144	0,27	0,02	59
Time at cortex (sec)				3,2	0,2	101			
KLP-7^{MCAK}(RNAi)									
cell type	SM			UMC					
population	total			total					
	mean	SEM	n	mean	SEM	n	mean	SEM	n
Growth rate (µm/sec)	0,18	0,01	308	0,10	0,003	149	0,11	0,01	65
Growth length (µm)	0,92	0,03	308	2,18	0,11	149	2,06	0,13	65
Growth duration (sec)	5,20	0,17	308	23,95	1,18	149	20,36	1,26	65
Shrinking rate (µm/sec)	0,57	0,02	293	0,63	0,02	156	0,62	0,03	66
Shrinking length (µm)	0,93	0,02	293	2,66	0,13	156	2,27	0,16	66
Shrinking duration (sec)	1,90	0,05	293	4,72	0,25	156	4,19	0,34	66
Catastrophe (sec-1)	0,19	0,01	308	0,04	0,002	149	0,05	0,003	65
Catastrophe (µm-1)	1,09	0,04	308	0,46	0,02	149	0,49	0,03	65
Rescue (sec-1)	0,53	0,01	293	0,21	0,01	156	0,24	0,02	66
Rescue (µm-1)	1,07	0,03	293	0,24	0,02	156	0,44	0,03	66
Time at cortex (sec)				10,0	1,1	96			

SEM: standard error of the mean. n = number of MTs. n(worms) ≥ 10

SUPPLEMENTAL EXPERIMENTAL PROCEDURES

C. elegans genetics

MDX12 was generated by crossing JJ1753 and NK682. JJ1753: unc-119(ed3) III; zuIs151 [pJN326: nmy-2::mRFP; unc-119(+)] was kindly provided by Jeremy Nance. NK682 contains an integrated transgene qyIs119 generated by amplifying the sequence of GFP-β-tubulin from pJH4.66 (pie-1p:: GFP::β-tubulin) and placing it after the *unc-62* promoter region, which was amplified from the fosmid WRM0629aH06. This transgene allows expression of GFP::tubulin in vulval epithelium and SM lineage through post-embryonic development to the adult stage (Jiang et al., 2009). MT dynamics were measured in the early embryo using MDX20, which was generated by out-crossing XA3501 (P*pie-1*::GFP::H2B ; P*pie-1*::GFP::*tbb-2*) with N2 males in order to isolate the transgene (*pie-1*::GFP::*tbb-2)*. The strain used for tissue specific RNAi was NK741: rrf-3(pk1426) II; unc-119(ed4) III; rde-1(ne219) V with an integrated transgene qyIs138 [Punc-62::RDE-1; unc-119(+); Pmyo-2::YFP].

Worm mounting and imaging conditions

Worms were anesthetized in 0.01% tetramisole in M9 buffer for 10 min before being transferred onto a 5% agarose pad. Worms were then covered with a poly-L-lysine coated coverslip. Coverslip was sealed with a mix of vaseline and paraffin wax and lanolin (1:1:1) and the imaging chamber was filled with M9 to prevent drying. To minimize out-of-focus light and maximize acquisition time, we used a real-time Swept Field Confocal (SFC, Nikon Canada, Mississauga, ON, Canada; and Prairie Technologies, Madison, WI, USA) using the 50 µm slit mode without binning on a CoolSnap HQ2 camera (Photometrics, Tucson, AZ). For Z-series and volume view, 60X or 100X/1.4 NA Plan-Apochromat objectives were used to acquire confocal Z sections with 500 µm steps. All SFC acquisitions and additional components including laser exposure setting were controlled by Elements software (Nikon). Acquisition of time-lapse for MT dynamics was performed with the 100X/1.4 NA Plan-Apochromat objective with the 1.5X optivar for 2 min with a time interval of 1 sec and less than 200 msec exposure time. A maximum of 5 movies (10 min of acquisition) were made on a single worm to avoid phototoxicity. At least 6 worms were imaged per condition.

SUPPLEMENTAL REFERENCES

Belmont, L.D., Hyman, A.A., Sawin, K.E., and Mitchison, T.J. (1990). Real-time visualization of cell cycle-dependent changes in microtubule dynamics in cytoplasmic extracts. Cell *62*, 579-589.

Cassimeris, L., Pryer, N.K., and Salmon, E.D. (1988). Real-time observations of microtubule dynamic instability in living cells. J Cell Biol *107*, 2223-2231.

Dhonukshe, P., and Gadella, T.W., Jr. (2003). Alteration of microtubule dynamic instability during preprophase band formation revealed by yellow fluorescent protein-CLIP170 microtubule plus-end labeling. Plant Cell *15*, 597-611.

Hanna-Rose, W., and Han, M. (2002). The Caenorhabditis elegans EGL-26 protein mediates vulval cell morphogenesis. Dev Biol *241*, 247-258.

Jiang, Y., Shi, H., and Liu, J. (2009). Two Hox cofactors, the Meis/Hth homolog UNC-62 and the Pbx/Exd homolog CEH-20, function together during C. elegans postembryonic mesodermal development. Dev Biol *334*, 535-546.

Lackner, M.R., Nurrish, S.J., and Kaplan, J.M. (1999). Facilitation of synaptic transmission by EGL-30 Gqalpha and EGL-8 PLCbeta: DAG binding to UNC-13 is required to stimulate acetylcholine release. Neuron *24*, 335-346.

Li, W., Miki, T., Watanabe, T., Kakeno, M., Sugiyama, I., Kaibuchi, K., and Goshima, G. (2011). EB1 promotes microtubule dynamics by recruiting Sentin in Drosophila cells. J Cell Biol *193*, 973-983.

Parsons, S.F., and Salmon, E.D. (1997). Microtubule assembly in clarified Xenopus egg extracts. Cell Motil Cytoskeleton *36*, 1-11.

Shelden, E., and Wadsworth, P. (1993). Observation and quantification of individual microtubule behavior in vivo: microtubule dynamics are cell-type specific. J Cell Biol *120*, 935-945.

Tanaka, E.M., and Kirschner, M.W. (1991). Microtubule behavior in the growth cones of living neurons during axon elongation. J Cell Biol *115*, 345-363.

Trent, C., Tsuing, N., and Horvitz, H.R. (1983). Egg-laying defective mutants of the nematode Caenorhabditis elegans. Genetics *104*, 619-647.

SUPPLEMENTAL MOVIE LEGENDS

Movie S1: Microtubule dynamics in the SM of a *C. elegans* larva expressing GFP-tagged tubulin, related to Figure 1.

Time-lapse imaging of a third larval stage (L3) *C. elegans* worm expressing GFP-tagged tubulin in the sex myoblast (SM) lineage and vulval precursor cells (not visible in this confocal plane). Images were acquired with 1 sec time interval at 150x magnification allowed visualization of MT dynamic instability in an intact developing nematode. Scale bar is 10 μm and playback rate is 15 times real time (15 frames per second).

Movie S2: Microtubule dynamics imaged in a uterine muscle cell (UMC) of an adult *C. elegans* worm expressing GFP-tagged tubulin, related to Figure 1.

Maximal projection of a 5 μm z-stack (600 nm interval) imaged every 10 sec in an adult worm expressing GFP-tubulin in the SM lineage. The movie represents MT dynamics in a differentiated uterine muscle cell (UMC). Scale bar is 10 μm. 1 frame (10 sec interval) is played every second: playback rate is 10 times real time.

Movie S3: Microtubule dynamics in a single confocal section in a uterine muscle cell (UMC), related to Figure 1.

GFP-tubulin is imaged in a single confocal section of the dorsal extension of a UMC where the cell is attached to its neighboring seam cell. The time lapse is made with 1 sec time interval at 150x magnification. MTs abruptly depolymerize when they encounter the cell border. This movie is decomposed in a montage in Figure S2, showing single and bundled MT tracks. Scale bar is 10 μm and playback rate is 15 times real time (15 frames per second).

Movie S4: Microtubule plus ends are oriented toward the cell periphery in the dorsal extension of the UMC, related to Figure 5.

The dorsal extension of a UMC in an adult worm expressing GFP-tubulin has been imaged every 10 sec on a swept-field confocal microscope. The movie represents a volume view of a z-stack (600 nm interval). MTs are oriented toward the cell edge where UMCs are attached to the seam cells. Scale bar is 5 μm and playback rate 10 times real time (1 frame per sec).

Movie S5: Microtubule organization and dynamics are perturbed by KLP-7^{MCAK} depletion, related to Figure 6.

Time-lapse imaging of MT dynamics in a single confocal plane of a uterine muscle cell (UMC) in a *klp-7 RNAi* worm. Images were acquired every second at 150x magnification. The area of the cell imaged is the cell border of the UMC dorsal extension where it attaches to the neighboring seam cell. KLP-7^{MCAK} depletion causes MT buckling. Scale bar is 10 μm and playback rate is 15 times real time (15 frames per second).